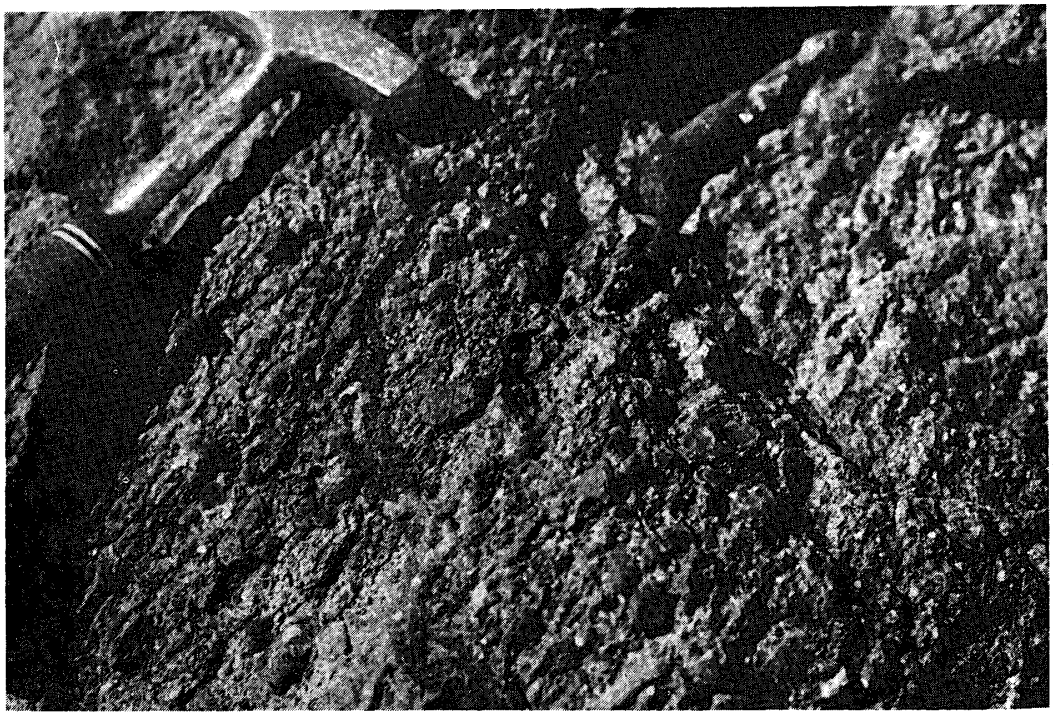

Fig. 14. Weathered surface of two-pyroxene syenite gneiss. Large dark-coloured potash feldspar porphyroblasts are shown.

Fig. 15. Schlieren-like contact of two-pyroxene syenite gneiss with clinopyroxene syenite gneiss.

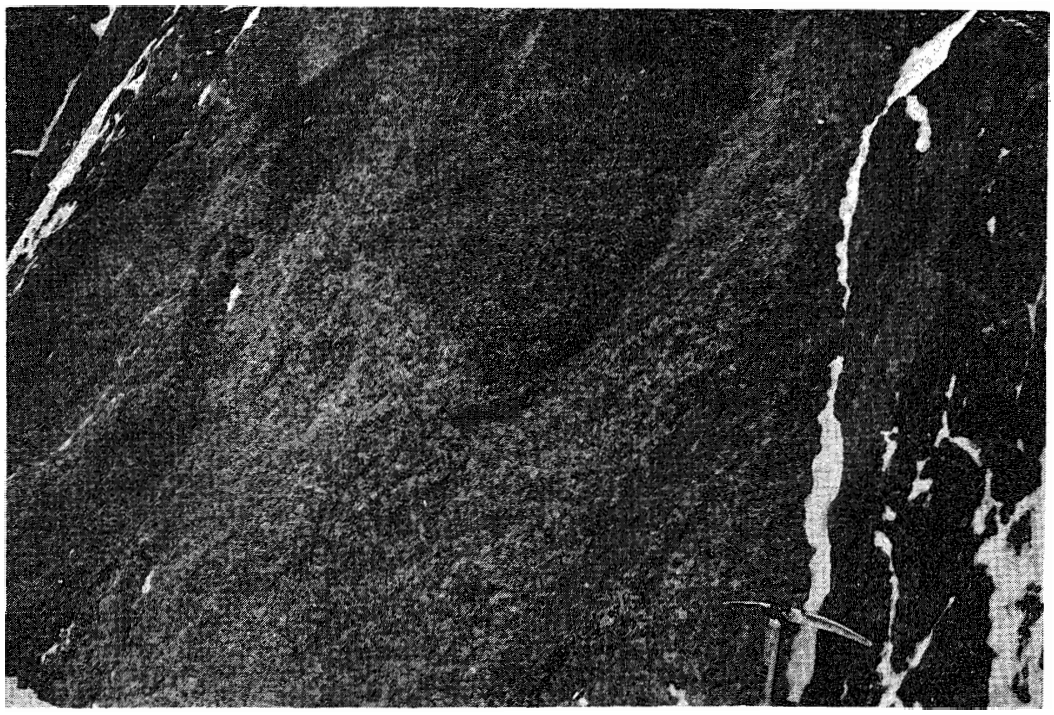

Fig. 16 Two-pyroxene syenite gneiss paleosome in clinopyroxene syenite gneiss.

Fig. 17. Schlieren gneiss of granite gneiss group.

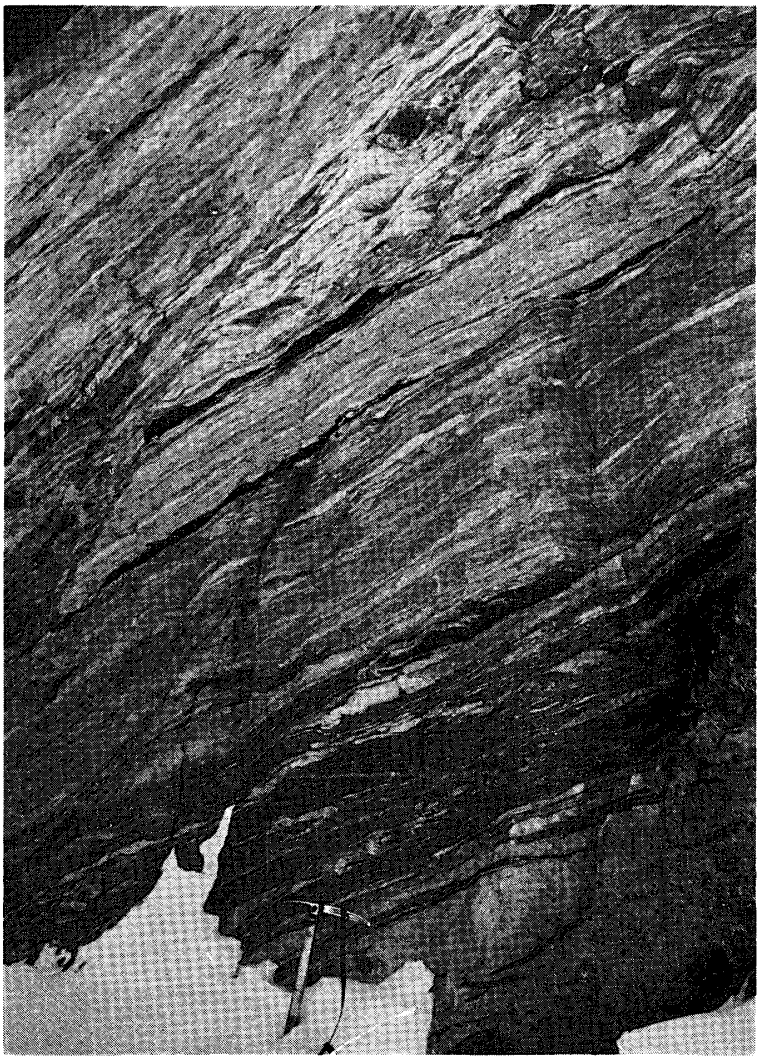

Fig. 18. Banded gneiss of granite gneiss group.

Fig. 19. Banded gneiss showing folded structure with gentle folding axis.

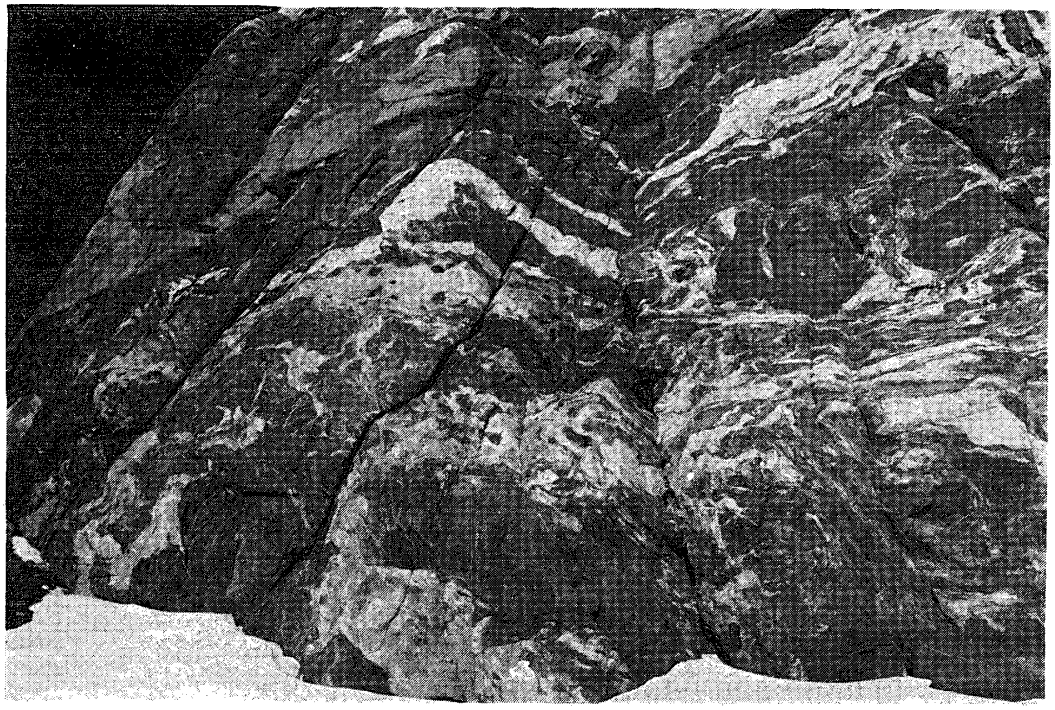

Fig. 20. Migmatite gneiss traversed by acid dyke at the latest stage.

Fig. 21. Close-up of migmatite gneiss showing schollen structure.

Fig. 22. Lit-par-lit injection of aplitic granite.

Fig. 23. Sheet-like aplitic granite in two-pyroxene biotite plagioclass gneiss.

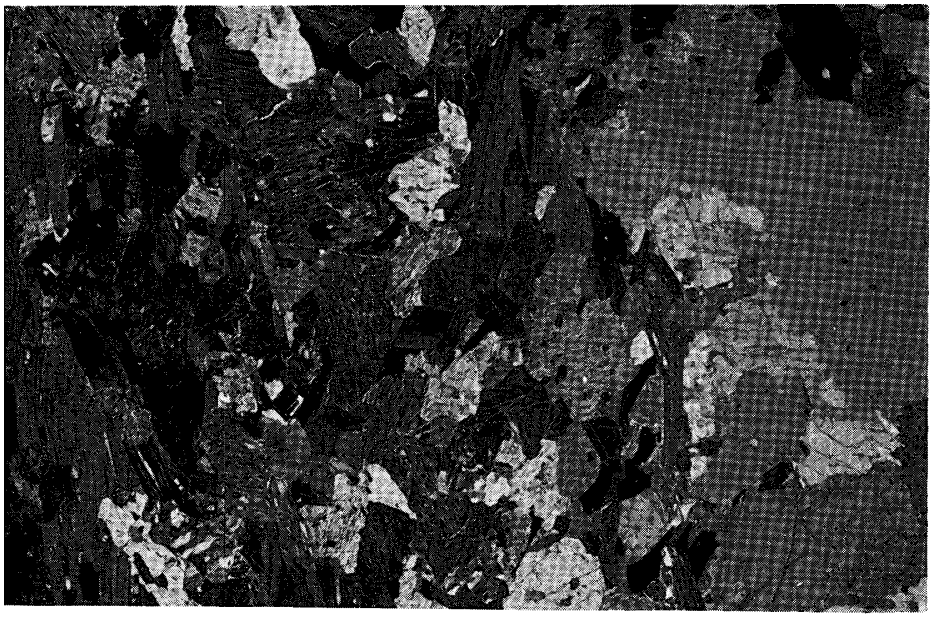

Fig 24. Two-pyroxene syenite gneiss (×8).

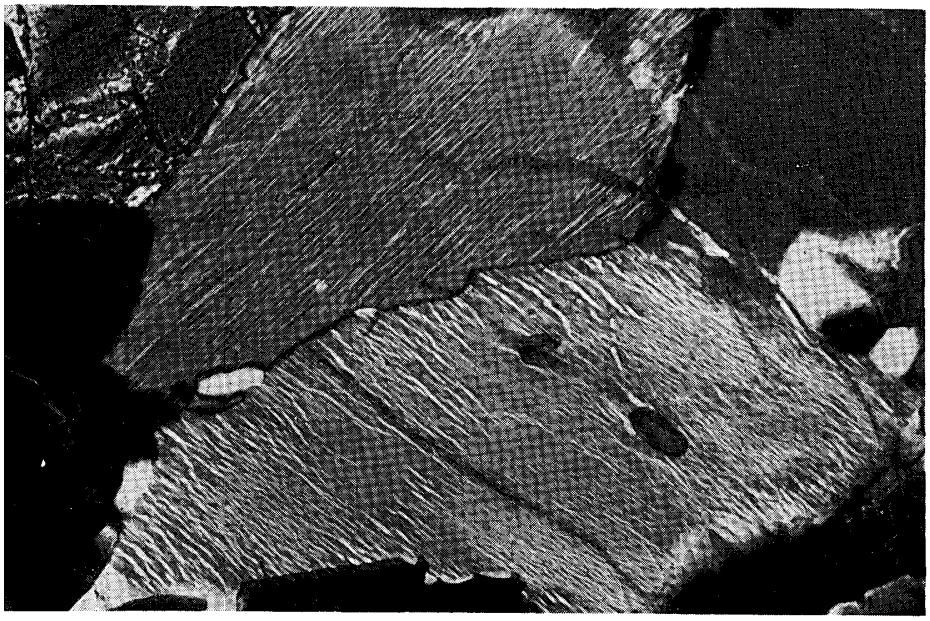

Fig. 25. Hair perthite in two-pyroxene syenite gneiss (×180)

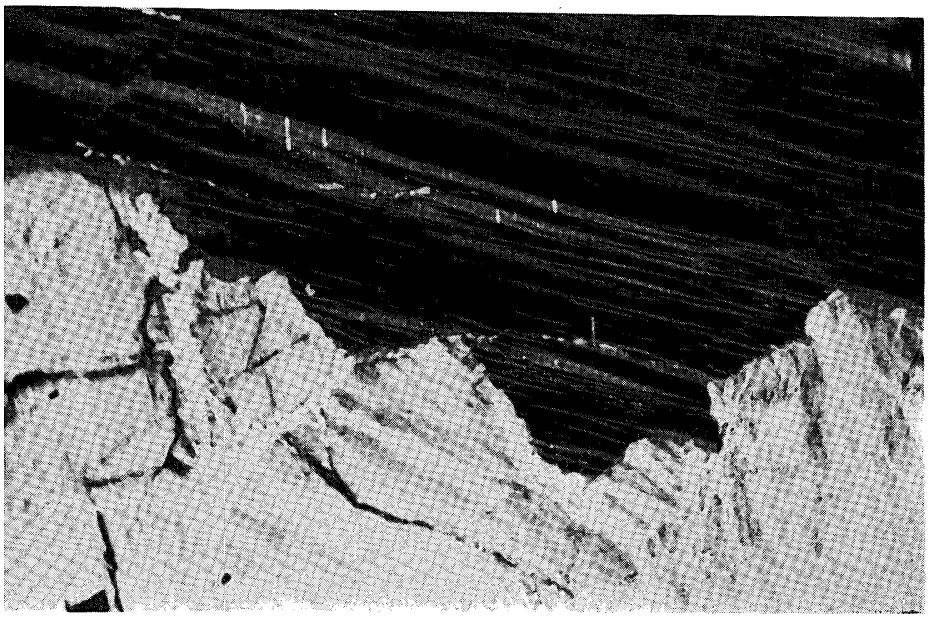

Fig. 26. Ribbon perthite in clinopyroxene syenite gneiss (×70).

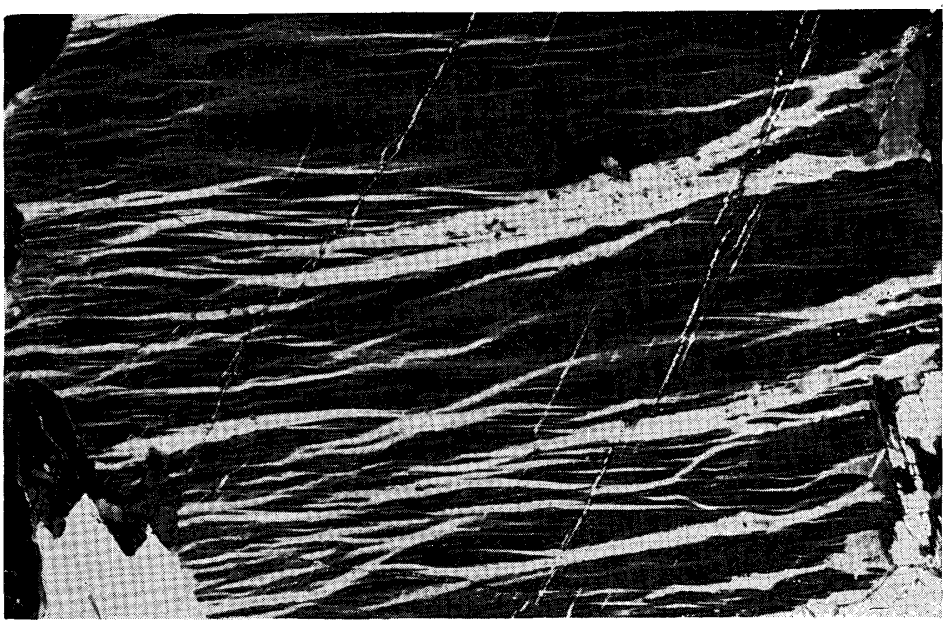

Fig. 27. Differently orientated hair and flame perthites (×70).

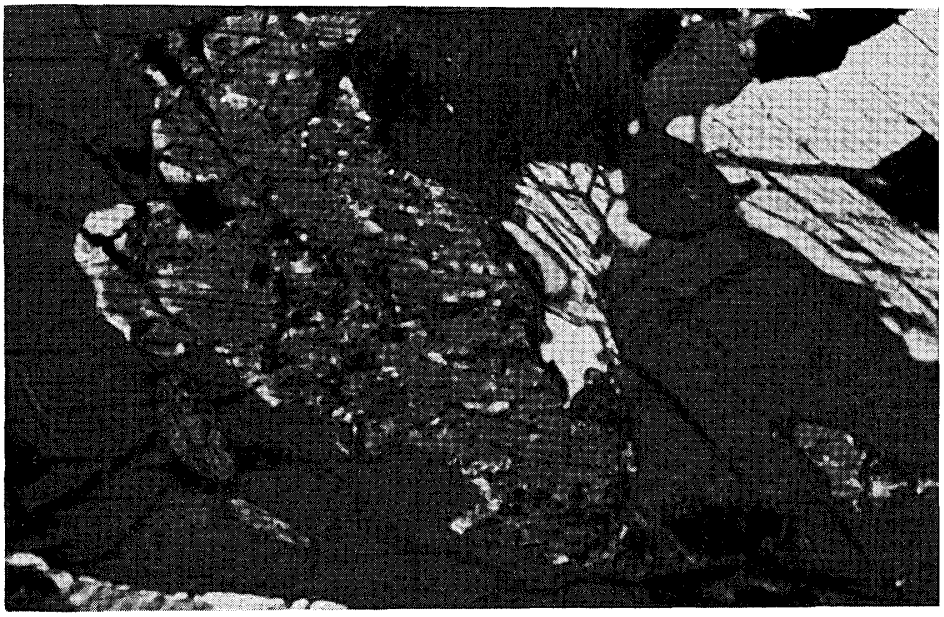

Fig. 28. Clinopyroxene altered to hornblende in clinopyroxene syenite gneiss (×70).

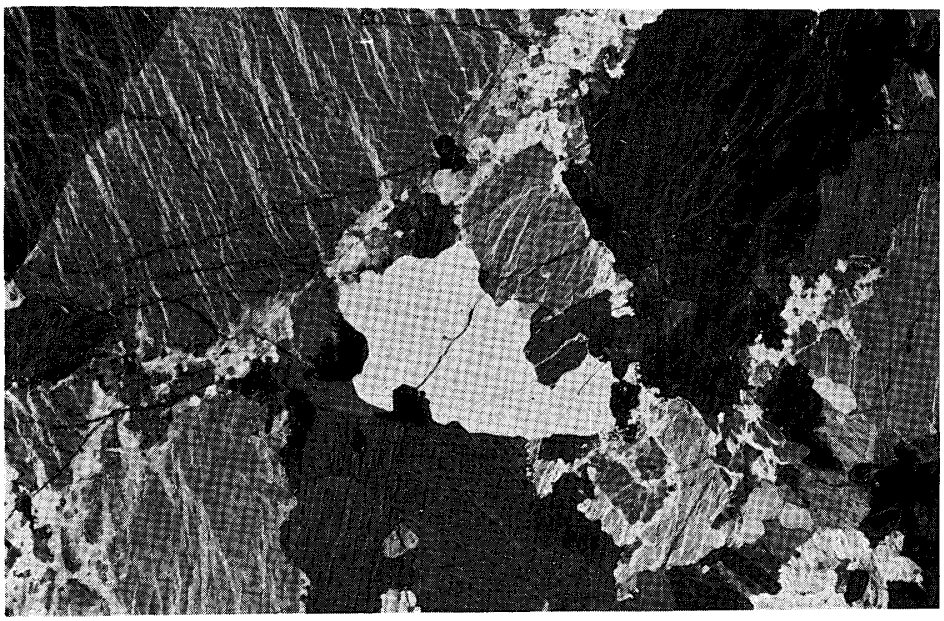

Fig. 29. Clinopyroxene quartz syenite gneiss (×8).

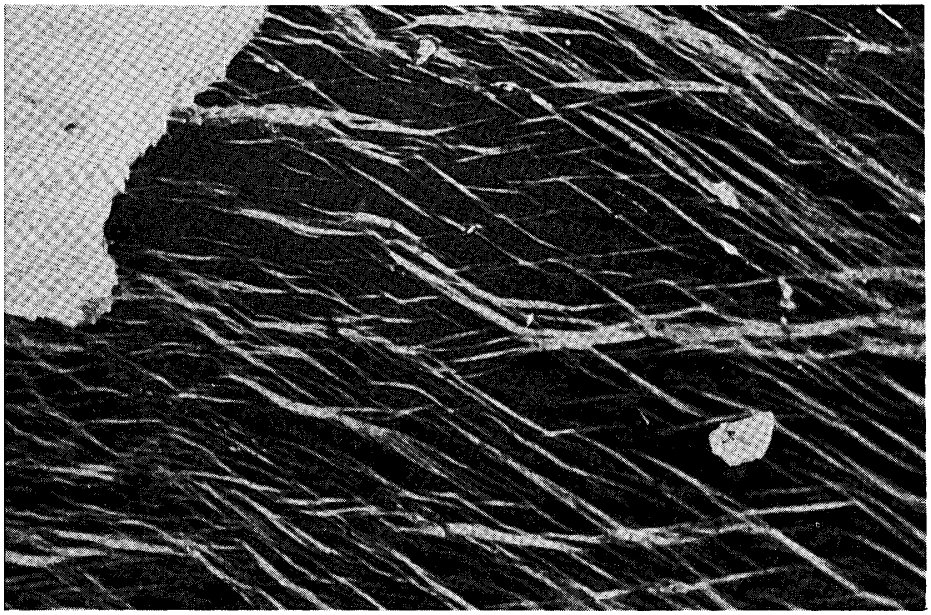

Fig. 30. Braid perthite in clinopyroxene quartz syenite gneiss (×70).

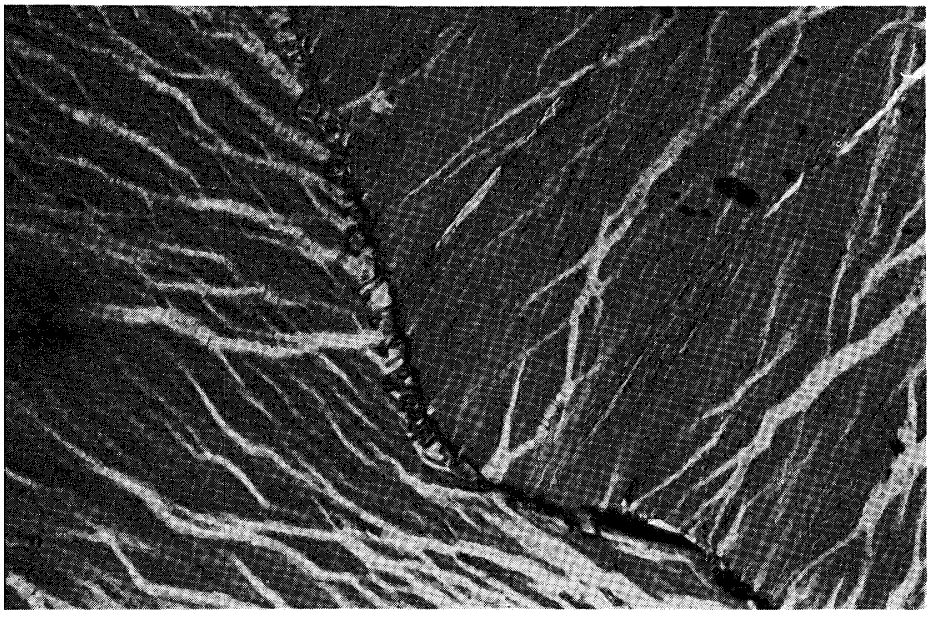

Fig. 31. Boundary relationship in flame perthite (×180).

Fig. 32. Biotite associated with sphene in clinopyroxene quartz syenite gneiss (×70).

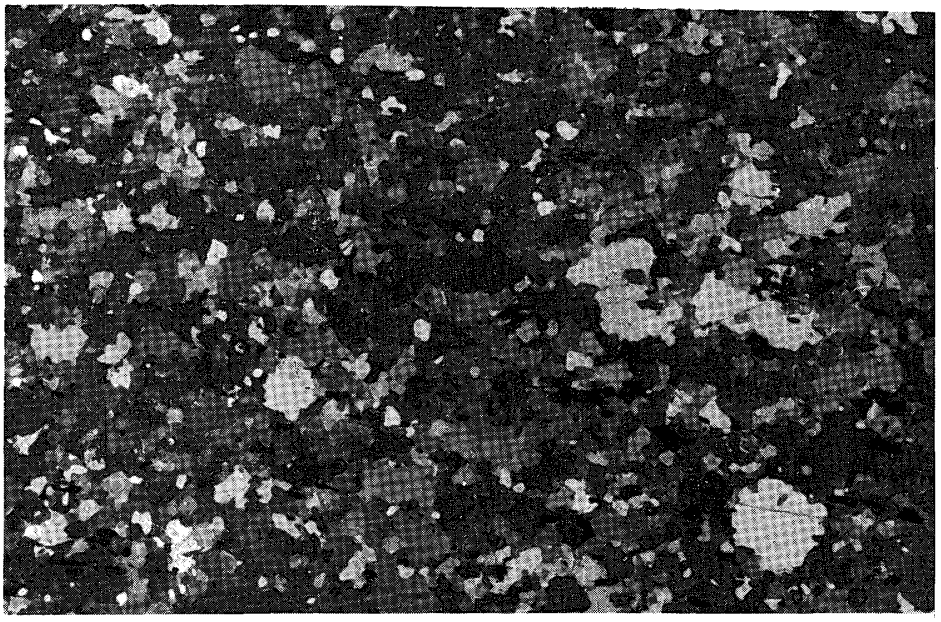

Fig. 33. Granite gneiss (×8).

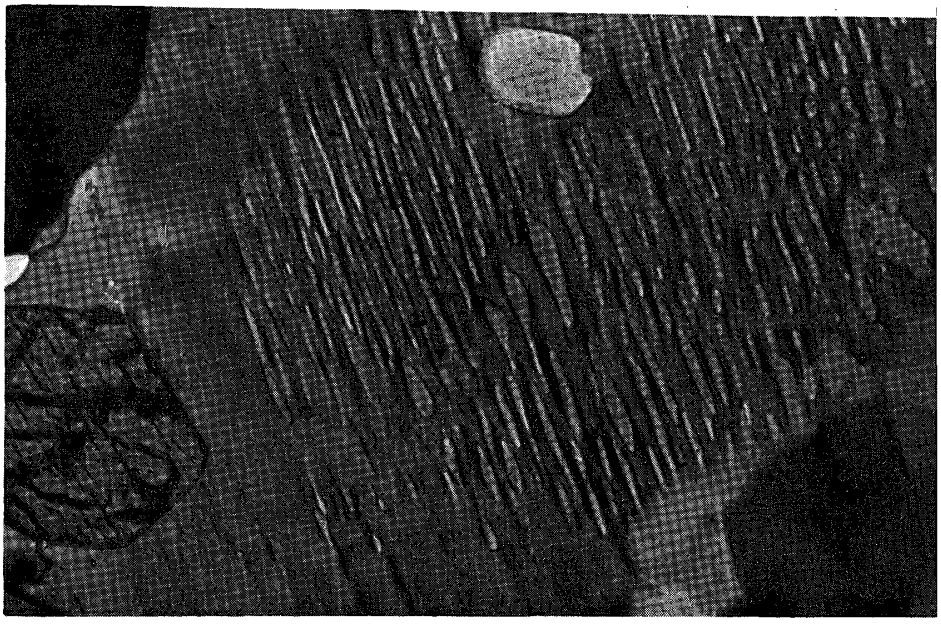

Fig. 34. Microcline perthite of stringlet type in granite gneiss (×180).

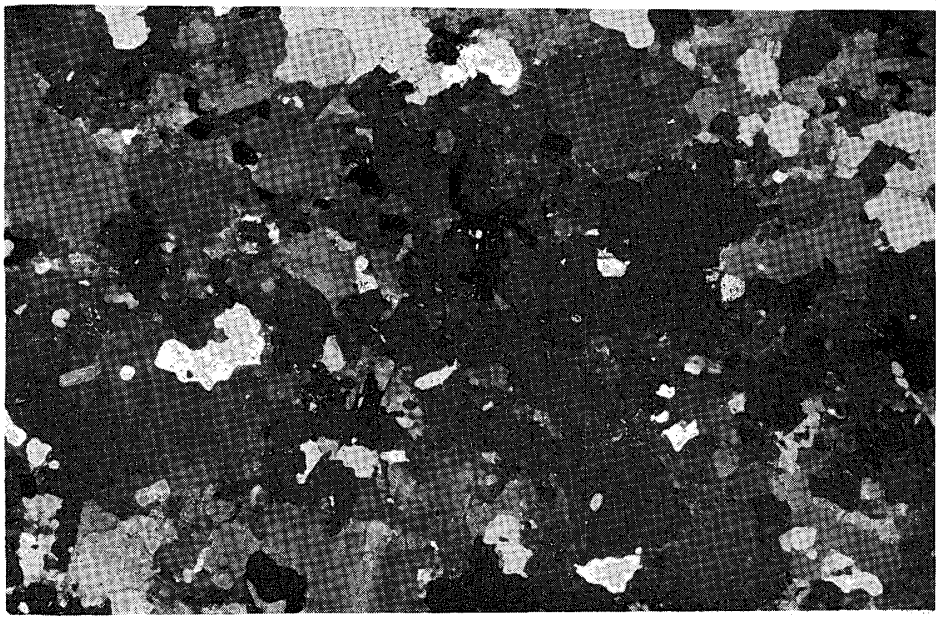

Fig. 35. Biotite granite (×8).

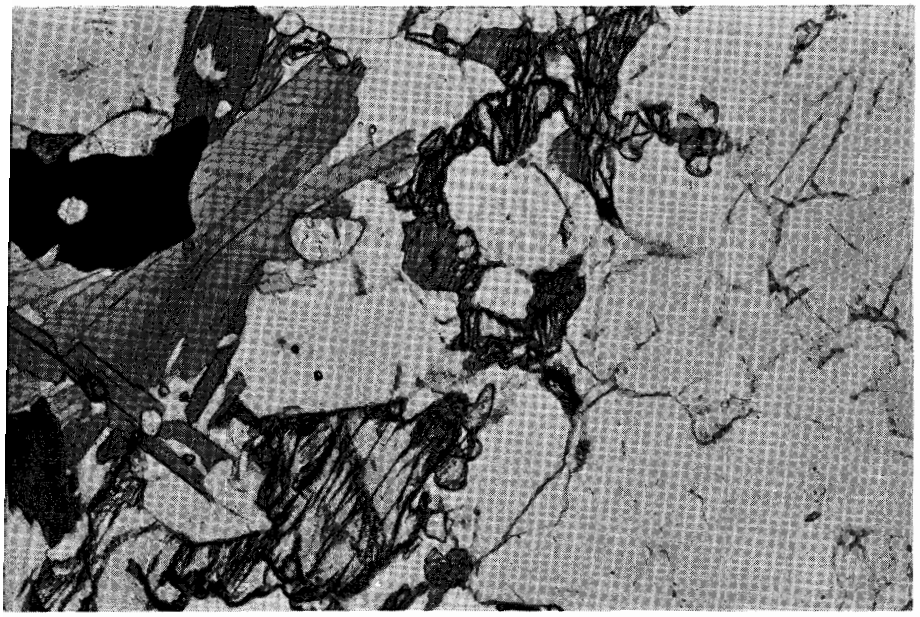

Fig. 36. Orthopyroxene in two-pyroxene biotite plagioclase gneiss (×70).

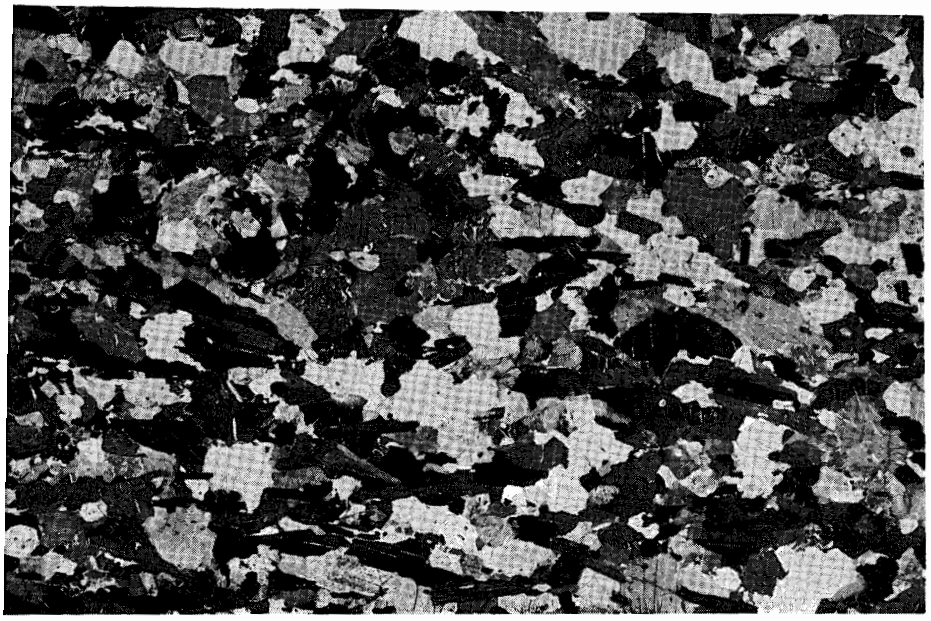

Fig. 37. Biotite granulite (×8).

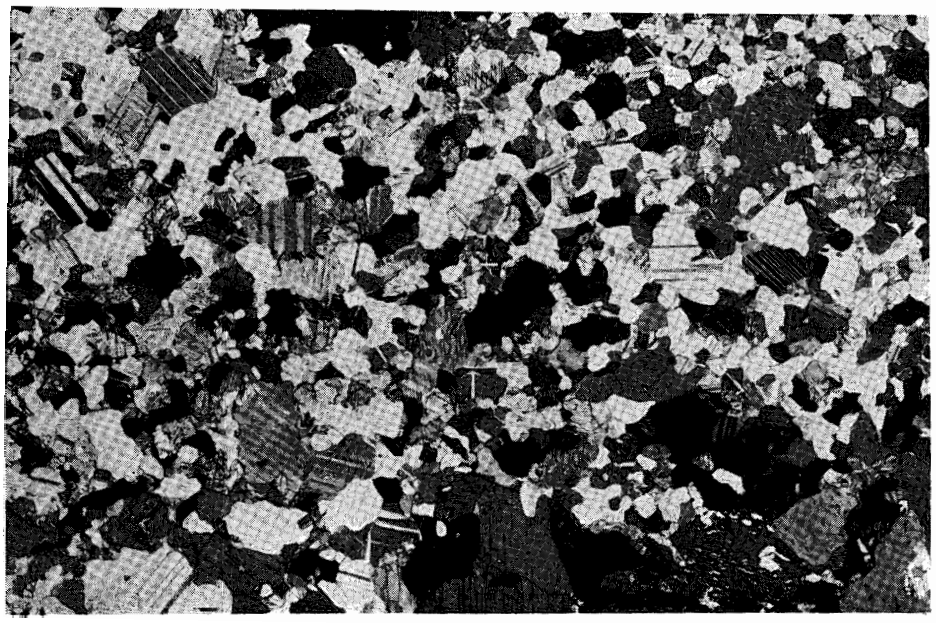

Fig. 38. Pyroxene amphibolite (×8).